Title
BRANCHING RATIO FOR PION-EETA DECAY: n+-> n| + e+ + v

Author
Bacastow, Robert B.

Publication Date
1963-06-10

University of California

Ernest O. Lawrence Radiation Laboratory

BRANCHING RATIO FOR PION-BETA DECAY: $\pi^+ \rightarrow \pi^0 + e^+ + \nu$

Berkeley, California

DISCLAIMER

Research and Development

UCRL-10864
UC-34 Physics
TID-4500-(19th Ed.)

UNIVERSITY OF CALIFORNIA
Lawrence Radiation Laboratory
Berkeley, California

Contract No. W-7405-eng-48

BRANCHING RATIO FOR PION-BETA DECAY: $\pi^+ \rightarrow \pi^0 + e^+ + \nu$

Robert B. Bacastow
(Ph. D. Thesis)

June 10, 1963

Printed in USA. Price $1.25. Available from the
Office of Technical Services
U. S. Department of Commerce
Washington 25, D.C.

BRANCHING RATIO FOR PION-BETA DECAY: $\pi^+ \rightarrow \pi^0 + e^+ + \nu$

Contents

BRANCHING RATIO FOR PION-BETA DECAY: $\pi^+ \rightarrow \pi^0 + e^+ + \nu$

Robert B. Bacastow

Lawrence Radiation Laboratory
University of California
Berkeley, California

June 10, 1963

ABSTRACT

A measurement of the $(\pi^+ \rightarrow \pi^0 + e^+ + \nu/(\pi^+ \rightarrow \mu^+ + \nu)$ branching ratio is a direct test of the conserved-vector-current theory of Feynman and Gell-Mann, and of Gershtein and Zeldovitch. We have measured this branching ratio by detecting the π^0-decay gammas and one of the gammas from the positron annihilation. The number of stopped pions counted was 5.6×10^{10} and the efficiency for detecting the $\pi^0 \rightarrow \pi^0$ decay was 0.32%. Five events were obtained with an estimated background of about one, giving a branching ratio of $(2.1^{+1.9}_{-1.2})\times 10^{-8}$ which is consistent with the value of 1.01×10^{-8} predicted in the conserved vector-current theory.

I. INTRODUCTION

The Conserved-Vector-Current (CVC) Theory was suggested independently by Feynman and Gell-Mann[1] and by Gershtein and Zeldovitch.[2] They noted the apparently curious coincidence that the vector and axial-vector coupling constants in muon decay are equal in magnitude to the vector coupling constant in beta decay, while the axial-vector coupling constant in beta decay is different; this can be summarized by

$$G_V^\mu = - G_A^\mu = G_V^\beta \ ,$$

and

$$G_A^\beta = - 1.2 \, G_V^\beta .$$

Recent experimental values of G_V^β from $O^{14}(\beta^-)N^{14}$ and G_V^μ from the muon lifetime differ by $(2 \pm 0.2)\%$,[3] but electromagnetic corrections to G_V^β are uncertain and could account for this small difference.[4] The equality in magnitude of the vector and axial-vector coupling constants in muon decay supports the idea of a universal weak interaction of the V-A type; the observation that the axial-vector coupling constant is changed in beta decay is not surprising, since strongly interacting particles are present. Virtual pion states formed by the strong interaction would not be expected to decay at the same rate as the "bare" particle states. The vector coupling constants being the same might be just a coincidence, or it might indicate that other interactions are arranged not to alter the coupling constant. In the electromagnetic interaction, virtual mesons do not alter the charge of particles because there is a conservation law for charge current:

$$\nabla \cdot \vec{j} + \frac{\partial \rho}{\partial t} = 0,$$

or, using 4-vector notation,

$$\partial \cdot j = 0 \ .$$

Feynman and Gell-Mann postulate a conserved weak current in analogy to the electric-charge current. The "universal" weak-interaction Hamiltonian is given by

$$H = \frac{G}{\sqrt{2}} J \cdot J^{+} ,$$

where

$$J_\mu = [\bar{p}\gamma_\mu(1+i\gamma_5)n] + [\bar{\nu}\gamma_\mu(1+i\gamma_5)e] + [\bar{\nu}\gamma_\mu(1+i\gamma_5)\mu]$$

is the weak current. With this current, the Hamiltonian has terms that describe all the familiar weak interactions involving nucleons, muons, and electrons. Consider now only the strongly interacting first term of the weak current. The vector part is

$$J_\mu^V = (\bar{p}\gamma_\mu n).$$

The electric-charge current is very similar, being

$$j_\mu = (\bar{p}\gamma_\mu p) = [\bar{\psi}\gamma_\mu(\frac{1}{2}+\tau_3)\psi] ,$$

where ψ represents the nuclear-wave function $(p\ n)$ in isotopic spin notation, and τ_3 represents the third component of the nucleon isotopic-spin operator. The nucleon isotopic-spin operator is

$$\tau_1 = \frac{1}{2}\begin{pmatrix} 0 & 1 \\ 1 & 0 \end{pmatrix} \quad \tau_2 = \frac{1}{2}\begin{pmatrix} 0 & -i \\ i & 0 \end{pmatrix} \quad \tau_3 = \frac{1}{2}\begin{pmatrix} 1 & 0 \\ 0 & -1 \end{pmatrix} .$$

To be conserved, the electric-charge current must include the pions because they also carry charge. We have

$$j_\mu = (\bar{p}\gamma_\mu p) + i\{[\pi^{+*}\partial_\mu\pi^{+} - (\partial_\mu\pi^{+})^{*}\pi^{+}] - [\pi^{-*}\partial_\mu\pi^{-} - (\partial_\mu\pi^{-})^{*}\pi^{-}]\}$$

$$= [\bar{\psi}\gamma_\mu(\frac{1}{2}+\tau_3)\psi] + i[\phi^{*}\tau_3\partial_\mu\phi - (\partial_\mu\phi)^{*}\tau_3\phi],$$

where

$\phi = (\pi^{+}\pi^{0}\pi^{-})$ is the pion-wave function in isotopic-spin notation, and the isotopic-spin operator for pions is

$$\tau_1 = \frac{1}{\sqrt{2}}\begin{pmatrix} 0 & 1 & 0 \\ 1 & 0 & 1 \\ 0 & 1 & 0 \end{pmatrix} \quad \tau_2 = \frac{1}{\sqrt{2}}\begin{pmatrix} 0 & -i & 0 \\ i & 0 & -i \\ 0 & i & 0 \end{pmatrix} \quad \tau_3 = \frac{1}{\sqrt{2}}\begin{pmatrix} 1 & 0 & 0 \\ 0 & 0 & 0 \\ 0 & 0 & -1 \end{pmatrix}.$$

Feynman and Gell-Mann postulate an analogous, conserved weak vector current which also includes the pions. Their postulated current is

$$J_\mu^V = \bar{\psi}\gamma_\mu\tau_+\psi + i\,[\phi^*\tau_+\,\partial_\mu\phi - (\partial_\mu\phi^*)\,\tau_+\phi].$$

The $\tau_+ = \tau_1 + i\tau_2$ operator gives charge changing weak currents as it must. The second term above was not formerly present and is the contribution of the Conserved-Vector-Current theory. There are now terms in the interaction which directly give the decay rate for

$$\pi^+ \to \pi^0 + e^+ + \nu\,.$$

This decay is expected in almost any theory through a diagram of the type shown below. The pion virtually forms a nucleon-antinucleon pair, one of the nucleons beta decays, and the other emits a π^0:

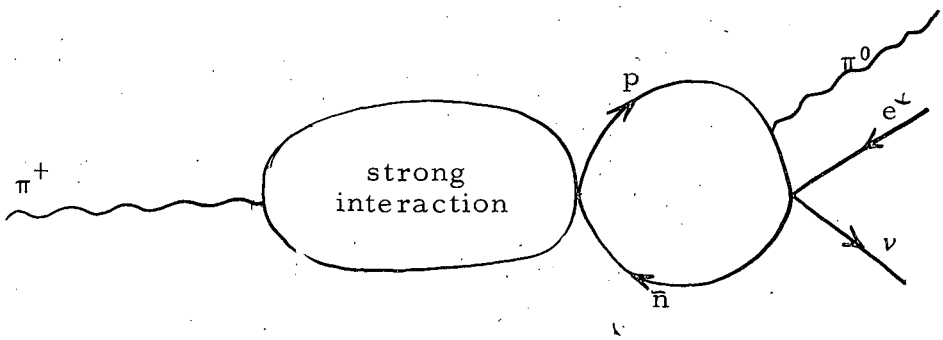

However, the CVC theory permits the direct calculation without introducing strong couplings and divergent integrals. The decay is a spin-zero to spin-zero transition so only the vector coupling contributes.

The interaction Hamiltonian which describes the π^+ decay is

$$H = \frac{G}{\sqrt{2}}\, i\,[\phi^*\tau_-\partial_\mu\phi - (\partial_\mu\phi)^*\tau_-\phi]\,[\bar{\nu}\,\gamma_\mu(1+i\gamma_5)e]$$

$$= Gi[\pi^{0*}\partial_\mu\pi^+ - (\partial_\mu\pi^0)^*\pi^+ + \pi^{-*}\partial_\mu\,\pi^0 - (\partial_\mu\pi^-)^*\pi^0\,]\,[\bar{\nu}\gamma_\mu(1+i\gamma_5)e]\,.$$

The decay rate λ can be very easily calculated if a few approximations are made. Using the "Golden Rule", we obtain

$$d\lambda = 2\pi \left| \langle H \rangle \right|^2 \delta (E_f - E_i),$$

and

$$\lambda = 2\pi \int \sum_{\text{spins}} \left| \langle H \rangle \right|^2 \delta(E_f - E_i) [d^3 p_e/(2\pi)^3] [d^3 p_\nu/(2\pi)^3].$$

The matrix element is

$$\langle H \rangle = \langle \pi^0, e, \nu \left| H \right| \pi^+ \rangle = \frac{G i (p_{\pi^+} + p_{\pi^0})_\mu}{\left(2p^0_{\pi^+}\right)^{1/2} \left(2p^0_{\pi^0}\right)^{1/2}} [\bar{u}_\nu \gamma_\mu (1 + i\gamma_5) u_e].$$

The π^+ decays at rest so $\vec{p}_{\pi^+} = 0$. If the π^0 recoil momentum is neglected compared to its mass, and if the $\pi^+ - \pi^0$ mass difference is neglected compared to the π^0 mass, the matrix element becomes

$$\langle H \rangle = G\, i\, \delta_{\mu 0} [\bar{u}_\nu \gamma_\mu (1 + i\gamma_5)\, u_e].$$

After squaring and summing over spins, we obtain

$$\sum_{\text{spins}} \left| \langle H \rangle \right|^2 = 2 G^2 (1 + V_e \cos \theta_{e\nu}).$$

The $\cos \theta_{e\nu}$ term is zero when integrated over the momentum angles so the rate involves only the phase-space integrals of ordinary beta decay, which are evaluated in most elementary nuclear physics books.[5] Again neglecting the π^0 recoil, we have

$$\lambda = (G^2 m_e^5/\pi^3) \int_0^{\eta_0} \left[(1+\eta_0^2)^{1/2} - (1+\eta^2)^{1/2} \right]^2 \eta^2 d\eta,$$

where $\eta_0 = p_e^{max}/m_e$. This gives the numerical result $\lambda = 0.415/\text{sec}$.

A recent value[3] of G_V^β and accepted values of the π^+ and π^0 masses[6] have been used: $G_V^\beta = (1.4025 \pm 0.0022) \times 10^{-49}$ erg cm^3, $m_{\pi^+} = 139.59$ MeV, and $m_{\pi^0} = 135.00$ MeV. The branching ratio is then

$$R = \frac{\lambda_{\pi^+ \to \pi^0}}{\lambda \pi^+ \to \mu^+} = (\lambda_{\pi^+ \to \pi^0})(\tau_{\pi^+}) = (0.415)(25.5 \times 10^{-9}) = 1.06 \times 10^{-8}.$$

The $\pi^- \to \pi^0$ rate (which is the same as the $\pi^+ \to \pi^0$ rate) has been calculated, without the approximations made above, by Da Prato

and Putzolu.[7] They also calculate electromagnetic corrections of 3.2%. Using the above value of G_V^β, their result is $\lambda = 0.395/\text{sec}$ and

$$R = 1.01 \times 10^{-8}.$$

The branching ratio to be expected if the CVC theory does not hold might be as much as a factor of 10 more or less than 10^{-8}, depending on the method employed in the calculation.[8-10]

During the past few years, considerable support for the CVC theory has come from experiments on beta-decay spectra and angular correlations. Mayer-Kuckuk and Michel[11] have compared the beta spectra from B^{12} and N^{12} as suggested by Gell-Mann.[12] The pion coupling with the electron and neutrino, in accordance with the CVC theory, predicts a modification to the transition-matrix element for beta decay. This modification is analogous to the contribution of the anomalous magnetic moment to gamma radiation, and it is of different sign for B^{12} and N^{12}, thus doubling the effect. The ratio of the transition-matrix elements for B^{12} and N^{12} is

$$|M(B^{12})|^2 / |M(N^{12})|^2 \approx (1 + AE),$$

where A is calculated to be $1.10 \pm 0.17\%$ in the CVC theory and 0.10% in the Fermi theory. Mayer-Kuckuk and Michel measure $1.30 \pm 0.31\%$, which is in agreement with the CVC theory.

Boehm, Soergel, and Stech[13] have measured a beta-gamma angular-correlation coefficient in the decay $F^{20}(\beta^-)Ne^{20*}(\gamma)Ne^{20}$ in agreement with the CVC theory. Nordberg, Morinigo, and Barnes[14] have measured beta-alpha correlation in the mirror-nuclei decays $L_i^8(\beta^-)Be^{8*}(\alpha)He^4$ and $\beta^8(\beta^+)Be^{3*}(\alpha)He^4$ and have found a difference in correlation coefficient again in agreement with the CVC theory. However, the comparison of these experiments with theory is less direct because of uncertainties in the calculation of certain nuclear-matrix elements.

A measurement of the $\pi^+ \rightarrow \pi^0$ branching ratio is probably the best and most direct verification of the CVC theory. However, the measurement of a branching ratio of 10^{-8} is not easy and its prospect

discouraged experimenters for several years. The $\pi^+ \rightarrow e^+ + \nu$ mode of decay occurs ten thousand times more often and yet was not discovered until 1958.[15]

In an experiment performed concurrently with the one described here, Depommier, Heintze, Mukhin, Rubbia, Soergel, and Winter have measured the $\pi^+ \rightarrow \pi^0$ branching ratio.[16] They report $(1.7 \pm 0.5) \times 10^{-8}$ in good agreement with the CVC theory. Dunaitsev, Petrukhin, Prokoshkin, and Rykalin[17] also believe they have detected the decay at a rate consistent with the CVC theory.

II. EXPERIMENTAL METHOD

A. Introduction

Our method of measuring the $\pi^+ \rightarrow \pi^0 + e^+ + \nu$ decay rate was to detect the two photons from the decay of the π^0, and the positron, and one of the photons from the annihilation of the positron. The π^0 decays almost instantly into two 67.5 MeV photons; because the energy available for the decay is small, these photons are nearly opposite (the angle between them differs from 180° by less than 3.8°). The positron has an energy between 0 and 4 MeV, with an average of 2 MeV. It has a maximum range in plastic scintillator of about 2 cm, and annihilates with an electron in materials similar to scintillator to give two opposite 1/2-MeV photons, within approx. 1 nsec.[18]

The two photons from the decay of the π^0 were detected by two opposite gamma counters. Each gamma counter was a stack of alternate layers of scintillator and lead. To reduce the background from random low-energy neutrons, the lead-scintillator stack was arranged so that alternate layers of the scintillator would be viewed by two different photo tubes. The two tubes were put in coincidence, to require that a proton scattered by a neutron would have to penetrate at least one layer of lead to simulate a photon conversion. For 3/32-in. lead sheets, the proton must have an energy greater than 35 MeV. Simple calculations based on equations given by Rossi[19] for energy loss of electrons by bremsstrahlung and ionization, and calculated curves given by Wilson[20] indicated that at least one of a pair of conversion electrons from a 70-MeV photon would have a good probability of penetrating the next sheet of lead. Nine pair of gamma counters were placed around a pion stopper to count the π^0 photons. Together, the gamma counters covered about one-half of the total solid angle.

The pion stopper was a scintillation counter in which the pion beam stopped. It detected the stopping pion and also the decay positron if these two events occurred with sufficient separation in time. Anti-counters were located between the pion stopper and the gamma counters

to prevent a charged particle from being mistaken for a photon. A large NaI counter was positioned close to the pion stopper to count the positron annihilation photon.

When a pion stopped, an electronic gate was opened. If a coincidence between opposite gamma counters occurred during the time of the gate, a data-storage apparatus was triggered. All the gamma counters were interrogated and those that had pulses were recorded on magnetic tape. The NaI counter signal was photographed on a four-beam oscilloscope. Also on the oscilloscope were the stopping counter and the π^0 gamma counters, from which the time of the event could be measured. A 7090 computer processed the magnetic tape, list those counters with pulses, and indicated which events might have come from opposite, colinear photons.

B. Pion Beam

The pion beam was made by the 740-MeV external proton beam of the Berkeley synchrocyclotron. Pions were produced at 0° by a 50 gm/cm^2 polyethylene target. Figure 1 shows the experimental area, the magnet system, and the position of the counter array.

The magnet system was designed to achieve a high-intensity low-energy pion beam.[21] It consisted of two large bending magnets and a three-element quadrupole. The bending magnets had a vertical aperture of 7 5/8 in.; the entrance and exit quadrupole elements had a 12 in. aperture. The center element of the quadrupole was a Panofsky section 16 in. wide and 6 1/2 in. high. However, no special advantage was taken of the rectangular aperture and it might just as well have been the usual quadrupole element. The beam was enclosed in a vacuum system that was placed between the polyethylene target and the exit of the second bending magnet.

Optically, there was a horizontal and vertical focus at the center of the quadrupole. All of the vertical focusing was done by the bending magnets; the horizontal focusing was done by the entrance and exit sections of the quadrupole. The center section of the quadrupole acted as

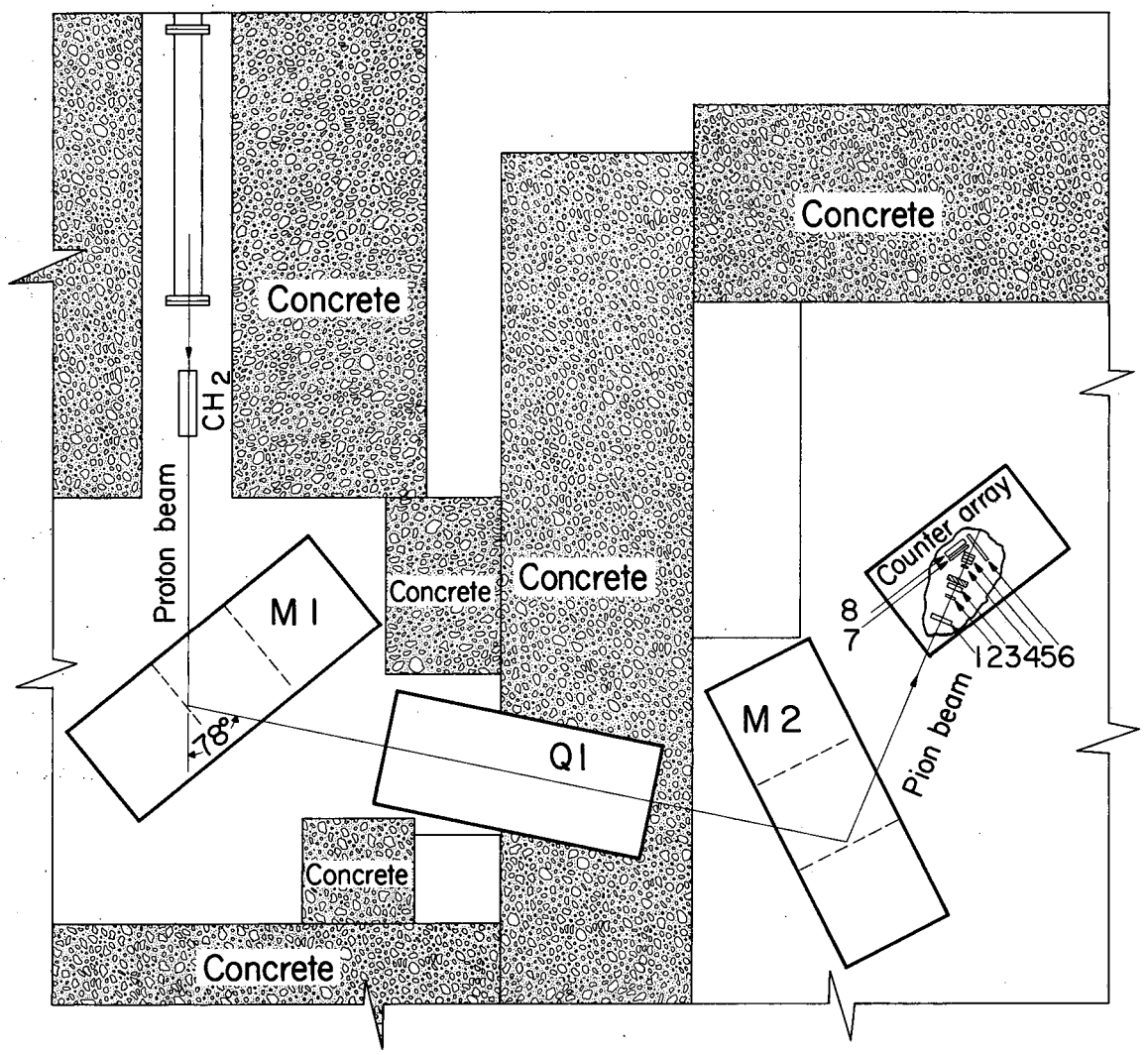

Fig. 1. Pion-beam magnet system and counter array.

a field lens vertically. The system achieves a large aperture and a short flight path for the pions. The short flight path is important if the pions are not to decay in the magnet system.

Considerable shielding was piled around the polyethylene target and a 3 ft-deep well was built into the back wall of the primary beam cave to stop the protons. A concrete blockhouse was built around the counter array and more shielding was put inside the blockhouse.

Horizontal and vertical beam profiles at the final focus were taken with two small counters mounted on a remote drive. Full width at half maximum was 2.0 in. in both the vertical and horizontal directions. Placement of carbon degrader corresponding to the counters and absorber used in the beam telescope during the experiment increased the beam width to about 3.0 in. The momentum spread of the beam was approximately ± 3% at half maximum.

The beam composition was measured using a time-of-flight technique over a flight path of 100 in.[22] The results are given in Table I. The data have been corrected for pion decay between the counters and for differences in multiple scattering in the first counter. Total charged particle flux through a 2-in. diam counter at full beam is also given. The numbers do not include protons because protons do not have enough range to go through the telescope at the momentum listed.

The Berkeley synchrocyclotron has an auxiliary dee that can be used to stretch the beam spill to about 12 msec out of the 16.7 msec of the acceleration cycle. However, the 54-nsec rf structure is still present. This stretched beam was always used.

Table I. Beam composition and flux (not including protons).

Momentum	Charged-particle flux per sec ($\times 10^5$)	Beam composition (%)		
		e^+	μ^+	π^+
100	2.8	--	--	--
150	4.7	62	12	26
175	6.2	40	17	43
200	7.7	36	~ 8	56
240	10.4	--	--	--

C. Counters

The location of the beam counters is shown in Fig. 2 and the counter sizes are given in Table II. Counters 2 and 4 defined the beam onto the pion stopper consisting of counters 5A, B, and C. Counter 5 was made in three sections, each with its own light pipe and phototube in order to reduce the stopping pion pulse relative to the decay-positron pulse. Between counters 3 and 4, and close to counter 3, was placed 10.0 g/cm^2 carbon absorber, so that the pions would stop in counter 5. Counters 6 and 7 were in anticoincidence with the other beam counters to indicate a stopped particle. Muons in the pion beam did not stop in counter 5, and were rejected by counters 6 and 7.

Counter 3 was a water Cerenkov counter to veto electrons in the pion beam which might scatter or shower in 5 and thereby simulate a stopping pion. The 175 MeV/c incident pions were just below the Cerenkov threshold for water when they reached counter 3. Counter 1 was used to discriminate against two beam pions in quick succession as they might simulate a real event through charge exchange of the second pion in the beam telescope; the operation of counter 1 will be explained in Section II-D.

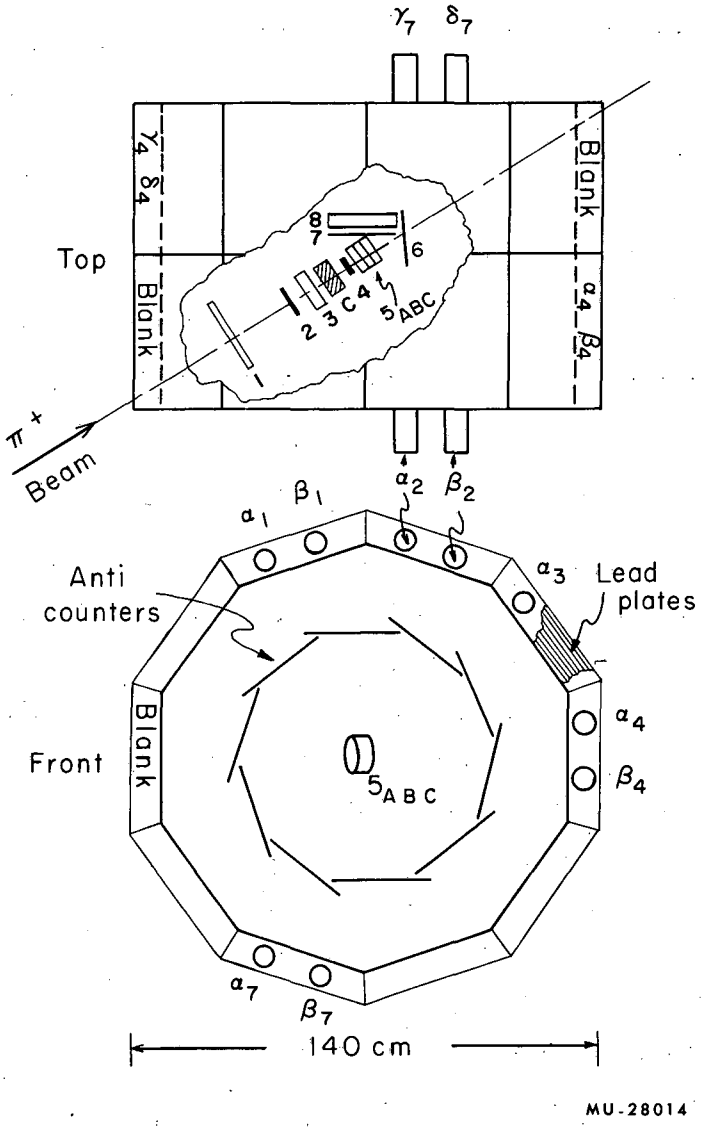

Fig. 2. Counter array.

Counter 8 was a thallium-activated sodium-iodide crystal. It was placed close to the stopping counter to count one of the 1/2-MeV photons from the positron annihilation. The crystal was 8 in. diam and 2 in. thick. It was purchased from the Harshaw Chemical Co., Cleveland 6, Ohio. A lucite light pipe connected it to an RCA 7046 photomultiplier tube.

To enable the beam-counter photomultipliers to operate at high currents (corresponding to particle fluxes of 4×10^5/sec), the voltages on the last 4 stages of the photomultiplier dynode structure were set by a resistor chain external to the tube base. A current high compared to that flowing in the dynodes could be maintained in the external resistor chain, and the dynode voltages thereby kept fixed even at a high counting rate.

The π^0 gamma counters were lead-scintillator sandwiches: 8 layers of 1/4-in. plastic scintillator were alternated with 8 layers of lead. The scintillator and lead sheets were 15.5×16 in. Alternate layers of scintillator were connected to two different phototubes. Figure 3 is a drawing of the basic unit. It shows 4 scintillators fastened to a common light pipe and phototube. Two units were interwoven to make one gamma counter. After they were interwoven, lead sheets were slipped between each pair of scintillators. During construction, each scintillator was wrapped with aluminum foil and covered with black cardboard before being glued to a common light pipe with three other scintillators.

Nine pair of gamma counters were built and they were arranged in two rings, one behind the other as shown in Fig. 2. In the first ring the two phototubes on each sandwich are referred to as α and β, on the second ring as γ and δ. The counters are numbered clockwise around the $\alpha\beta$ ring; the numbers on the $\gamma\delta$ ring are such that $(\alpha\beta\gamma\delta)_i$ denote opposite counters with respect to the pion stopper.

Except for counters $(\alpha\beta\gamma\delta)_1$ and $(\alpha\beta\gamma\delta)_6$, the gamma counters contained 3/32-in. (2.70 g/cm^2) lead sheets. Counters $(\alpha\beta\gamma\delta)_1$ contained 1/8-in. sheets and counters $(\alpha\beta\gamma\delta)_6$ contained 1/16-in. sheets.

Ten plastic-scintillator counters, A_i (i = 1 to 10), were placed between the pion stopper and the π^0 counters to veto counts that were

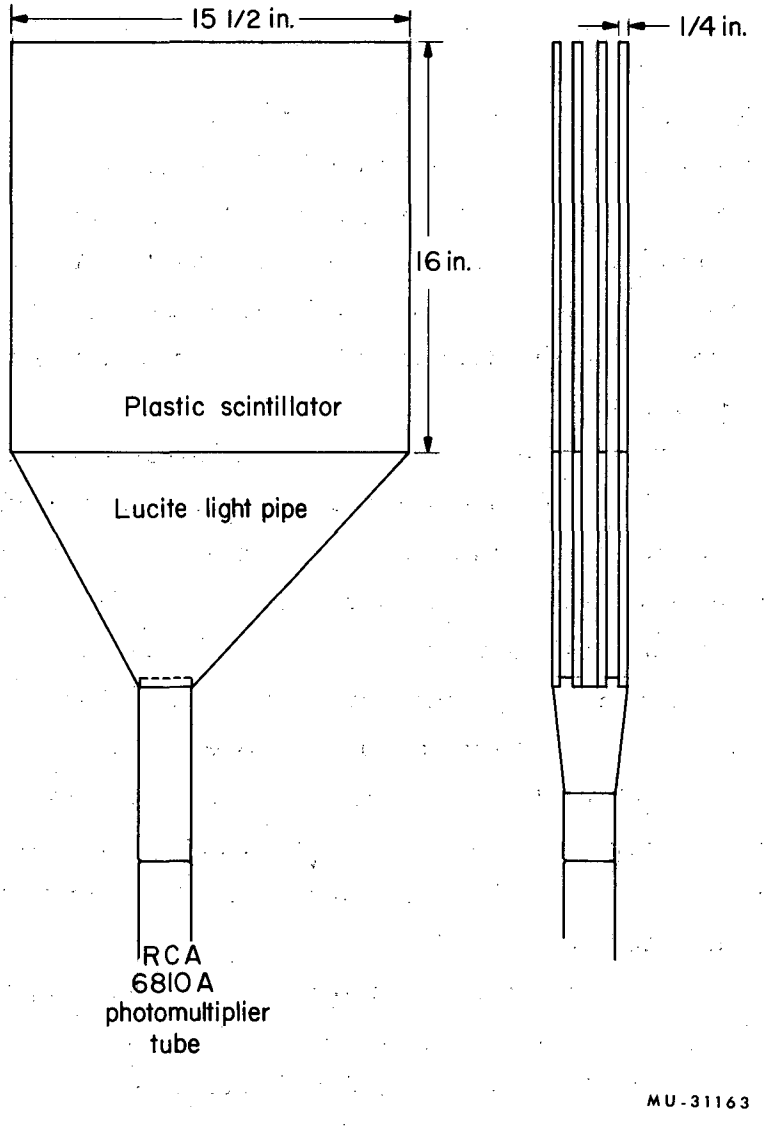

Fig. 3. Element of a π^0 gamma counter.

caused by charged particles. These counters were of dimension 3/8×11 3/4×34 in. and together completely shadowed the π^0 gamma counters from the stopper.

With the exception of the NaI counter, all the counters employed RCA 6810A photomultiplier tubes.

Table II. Beam-counter sizes.

Beam Counters	Size (in.)	Composition
1	1×7 diam.	plastic scintillator
2	5/8×4 1/2 diam.	plastic scintillator
3	1 1/4×5×5	water in copper tank
4	1/8×3 diam.	plastic scintillator
5A	1×3 1/2 diam.	plastic scintillator
5B	1×3 1/2 diam.	plastic scintillator
5C	1×3 1/2 diam.	plastic scintillator
6	1/4×7 diam.	plastic scintillator
7	3/8×8 1/4 diam.	plastic scintillator

D. Electronics

A block diagram of the electronics is given in Fig. 4. A pion stopping in counters 5A, B, or C, generated the signature ($2\,4\,5A\,\overline{3}\,\overline{6}\,\overline{7}\,\overline{1D}$). The 1D signal occurred if another beam particle entered the system within an interval of 10 to 60 nsec following the pion stop. Consequently, $\overline{1D}$ demanded that no other beam particle enter the system during the time we awaited a possible $\pi^+ \rightarrow \pi^0$ decay. To make the 1D signal, the 1 pulse was split, one part opened gate 1 so that a pulse on the other half of the split 10 to 60 nsec later would go through the gate. Gate 2 was made to act as a pulse stretcher by using the gate monitor as the output.

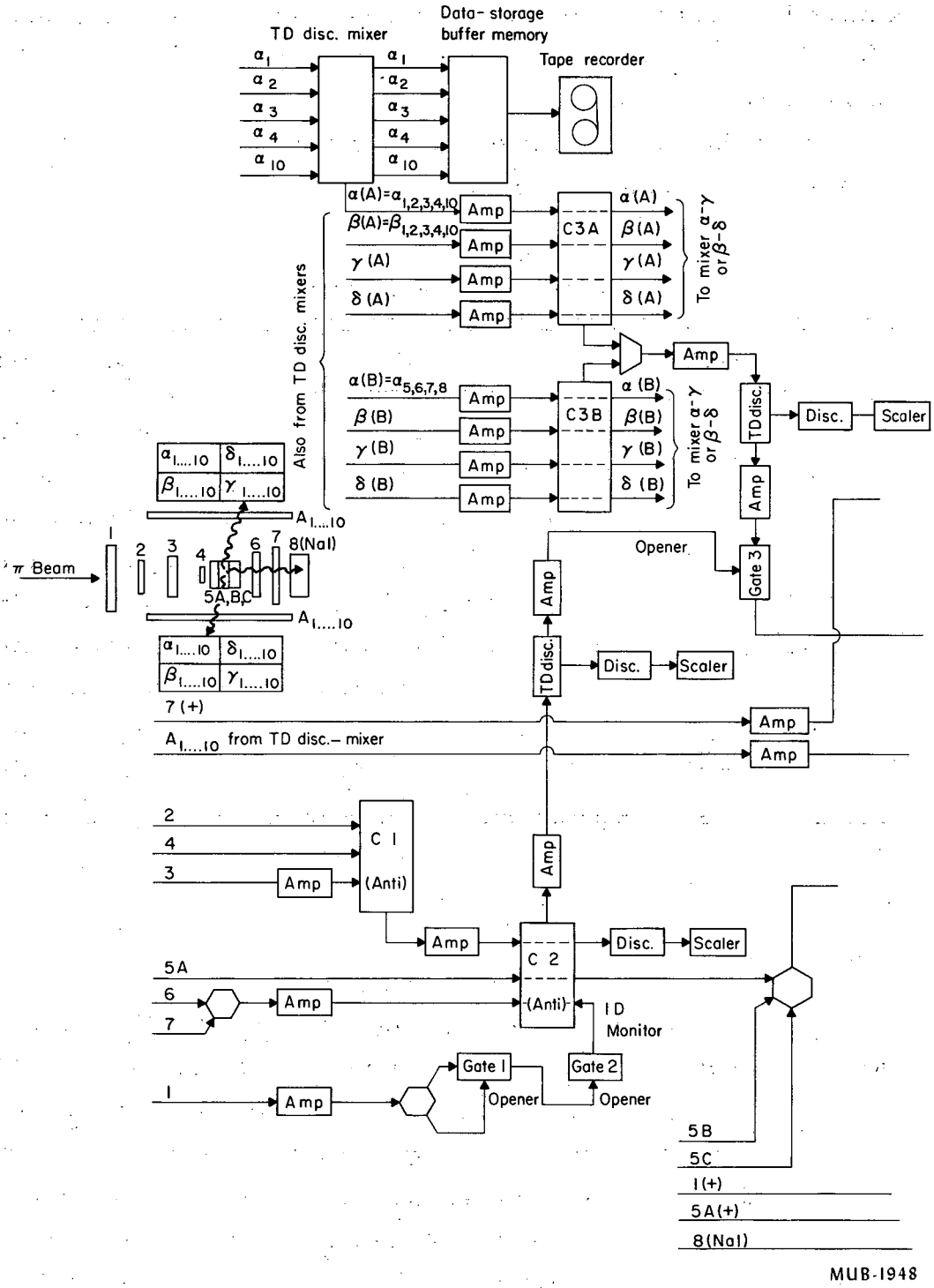

Fig. 4. Diagram of the electronics.

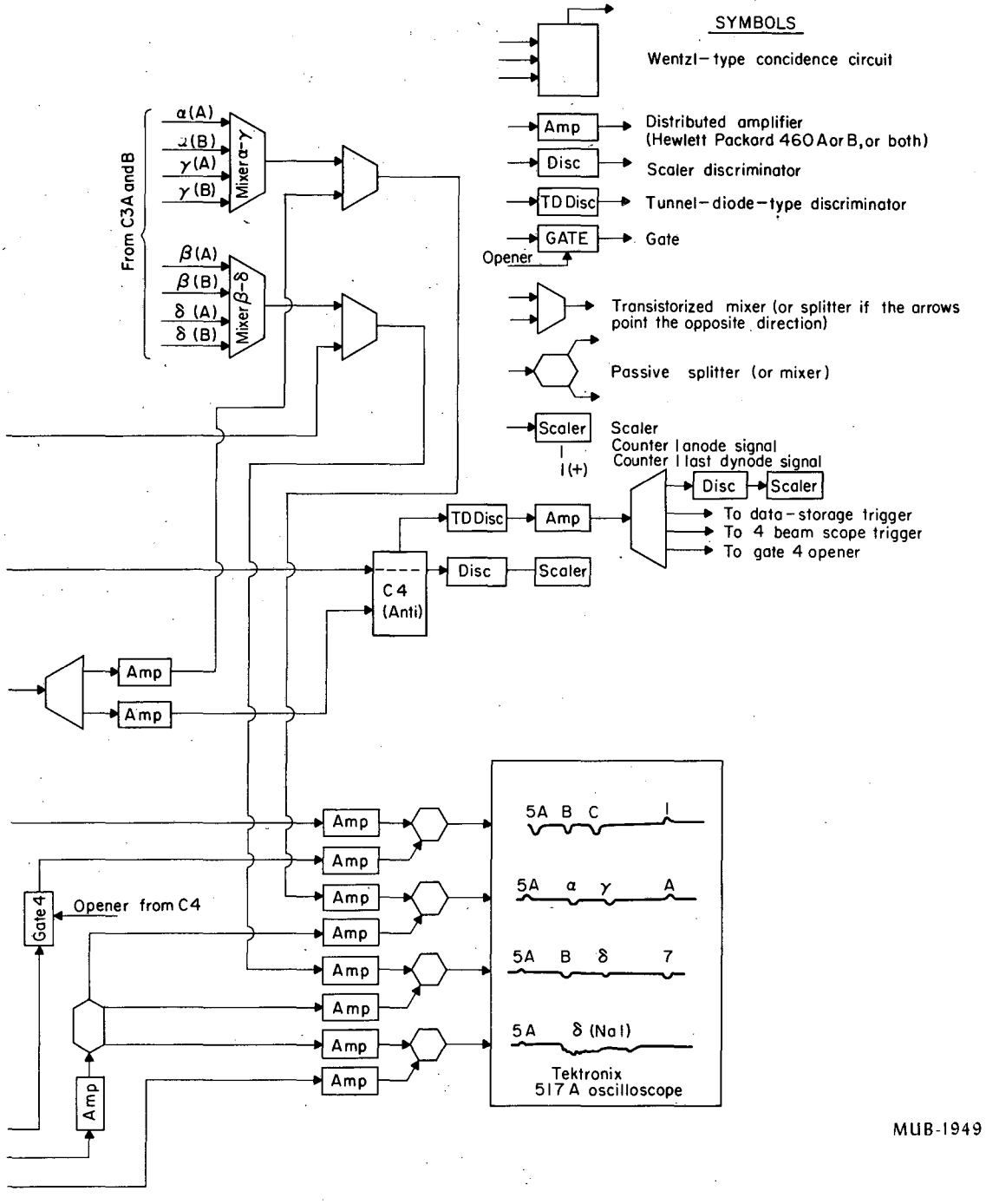

Fig. 4. Diagram of the electronics.

The output from each of the gamma counters and from the anti-counters $A_{1...10}$ went to tunnel-diode discriminator circuits.[23] Two sets of signals were taken from the discriminators. One set consisted of the individual, discriminated outputs and went to the magnetic-tape data-storage apparatus. The other set contained the mixed signals and went to the C3 coincidence circuit.

Each of the two rings of counters, $\alpha\ \beta$ and $\gamma\ \delta$ were further divided into two sections, A and B. Section A contained counters 1, 2, 3, 4, and 10; B contained counters 5, 6, 7, and 8. The A and B coincidences were made separately in C3A and B, and then mixed. This arrangement reduced the trigger rate as compared to an arrangement bringing all the gamma counters into one circuit.

The C3 output went through gate 3, which was opened by the stopping pion signal, and into C4, where it was stopped if there was a signal from any of the anticounters $A_{1...10}$. The C4 output triggered the data storage system and the four-beam oscilloscope.

The four-beam oscilloscope display is also shown on Fig. 4. On this drawing, α is meant to represent the sum of all the α counters, and similarly for β, γ, δ, and A. The 1 signal on the oscilloscope display went through gate 4, opened by the C4 output for about 80 nsec, because otherwise the 5A, B, and C displays were too often spoiled by an earlier 1 pulse. The signal from 7 was included on the display to rule out NaI pulses from charged particles originating in the stopper. The 5A pulse was put on each trace as a timing marker. All timing measurements were made with respect to these pulses to eliminate errors arising from jitter or drift in the time at which each trace started.

The film was projected onto the ground-glass screen of a viewer produced by Documat, Inc., of Belmont, Mass. The magnification of the oscilloscope trace was 5.0. The oscilloscope-sweep speed was ordinarily 100 nsec/cm so one cm on the screen corresponded to 20 nsec.

The data-storage apparatus is described in detail by Wiegand,[24] and Evans and Kirsten.[25] It consisted of a magnetic-core buffer memory and a tape recorder. Ten events were stored in the memory and then read out. During the write out, an event could not be stored, so a gate

pulse was generated which blocked the C1, C2, and C3A and B output pulses. The gate pulse turned off the bias voltage to the tunnel-diode discriminators following C2 and C3A and B, and the voltage to the C1 scaler discriminator. Each stored event was numbered, and a pulse was generated which advanced a register which was photographed along with the four-beam oscilloscope display. In this way each event was labelled with the same number in the data storage and the oscilloscope display.

E. Procedure

In this section, methods of setting voltages, delays, etc., are discussed.

The gamma counters were timed with a light pulser.[26] A light pulse in 5A opened gate 3 (Fig. 4) and another simultaneous light pulse in a γ counter made a signal which went through gate 3. The fraction of the counts going through the gate as a function of gate delay was recorded. By noting for each counter the relative time of the sharply rising leading edge of the gate, the relative delay of all counters could be easily made the same within 1.0 nsec.

All the tunnel-diode-discriminator mixers were set to accept a pulse of 180 mv or greater. The voltages of all the gamma counters were set so that they counted the same when exposed to a Na^{22} source. The final voltages were set by using π^0's made from stopping π^-'s in counter 5. A small fraction of the pions were captured by hydrogen and gave π^0's through the reaction $\pi^- + p \rightarrow \pi^0 + n$. The data-storage apparatus was a great help in setting the voltages because 9 of the 36 counters could be varied simultaneously. A 7090 computer summarized the data. The timing of all the counters was redone after setting the voltages.

The timing and length of gate 3 was also measured with π^0's from stopping π^-'s. Figure 5 shows this curve; the times are relative to the normal operating point during the experiment. A pion decay curve is also shown to indicate the fraction of pions which decay within the gate.

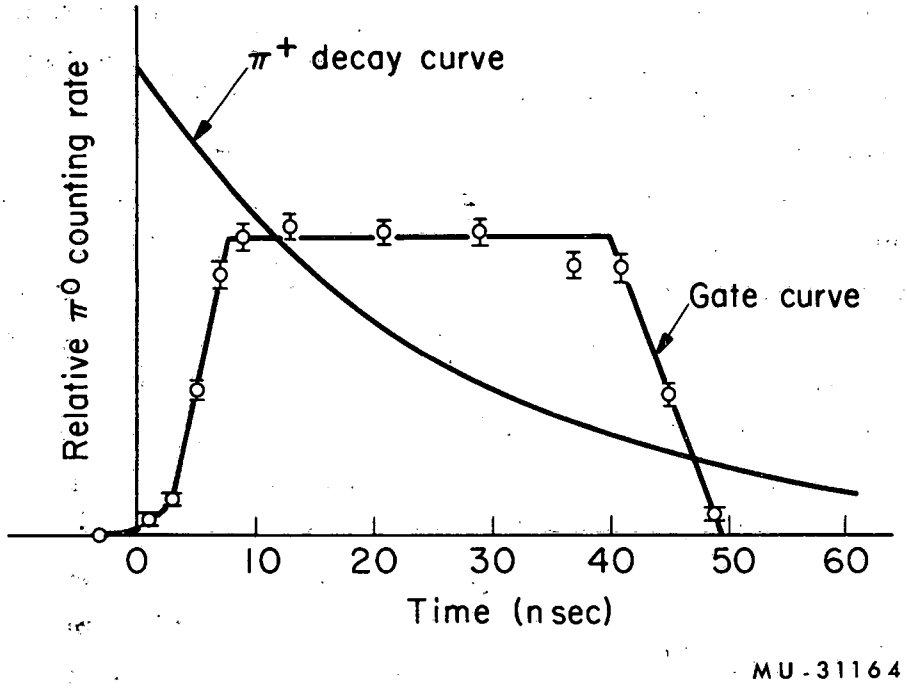

Fig. 5. Timing and length of Gate 3. The gate curve was made with π^0's from stopping π^-'s. The normal operating point during the experiment was at 0 time. A π^+ lifetime curve is shown to indicate the timing efficiency of the gate.

The location of the γ counters on the four-beam oscilloscope display was found also with π^0's from stopping π^-'s. This gave the locations for prompt events; the displacement from these locations gave the time of the event.

The incident momentum of 175 MeV/c was chosen by making a compromise between the pion stopping rate, which was highest at about 200 MeV/c, and the data-storage trigger rate, which decreased with decreasing incident momentum. The stopping pion rate was about 15% higher at 200 MeV/c, but the π^0 trigger rate was twice as high. The apparent reason that the trigger rate was sensitive to the beam energy is that the charge-exchange cross section increases sharply with energy for low energy pions.[27]

III. EFFICIENCY

A. Introduction

To obtain the beta-decay branching ratio, the absolute efficiency to detect the reaction must be known. The overall efficiency is the product of many factors, some measured and others calculated. Table III itemizes the partial efficiencies, and they are all discussed in further detail below. The overall efficiency for counting the π^0 photons and the positron annihilation photon is $(0.35 \pm 0.12)\%$; if the electron is also counted, the overall efficiency is further multiplied by 0.51.

B. Gate Timing Efficiency

An electronic gate was opened at 5 nsec, and closed at 45 nsec, after the pion stopped. Only if a four-fold coincidence of the π^0 counters occurred during the gate was an event recorded. Figure 5 shows the gate curve and an exponential decay curve for the pion (25.5-nsec mean life). Because 65% of the pions decayed within the gate, the timing efficiency is 0.65. If the gate was positioned to include zero time, or lengthened, the number of triggers were increased, making the data analysis more difficult.

C. π^0 Efficiency

The π^0 efficiency is obtained from a measurement made at CERN of the number of π^0's produced per π^- stop in CH. The efficiency can also be directly calculated but the calculation is uncertain because it includes an electronic efficiency that is not well understood.

Chabre et al.[28] have reported that $(5.4 \pm 0.5) \times 10^{-3}$ π^-'s are captured by the hydrogen of CH per π^- stop in CH. By using the Panofsky ratio,[29] one obtains

$$(1.5/2.5)(5.4 \pm 0.5) \times 10^{-3} = (3.2 \pm 0.3) \times 10^{-3}$$

π^0's produced per π^- stop in CH. Dunaitsev et al[30] have reported a ratio of 290 ± 40 π^0's from a liquid-hydrogen target to π^0's from a CH_2 target. The ratio of π^0's from a hydrogen

Table III. Efficiency summary.

Gate timing		0.65
π^0 photon efficiency		
Solid angle	0.43	
Probability that photons hit opposite counters	0.85	0.044
γ-counter efficiency (for pair)	0.12	
Annihilation photon efficiency		
Solid angle	0.35	
Counter efficiency	0.74	0.14
Conversion in stopper	0.78	
Interference from another pulse	0.70	
Positron efficiency		
Energy greater than 1/2 MeV	0.93	0.51
Detection efficiency	0.55	
Accidental anticoincidence		0.92
Film not readable		0.95

Table IV. Resolution factors calculatted by the Monte-Carlo Method; R is the probability that the decay photons from a π^0 hit opposite counters.

Source of π^0	Counters	R
π^+ decay	$(\alpha\ \beta\ \gamma\ \delta)_i$	0.76
π^+ decay	$(\alpha\ \beta)_i\ (\gamma\ \delta)_j$, $j = (i+1)$ or $(i-1)$	0.06
π^+ decay	$(\alpha\ \beta)_i\ (\gamma\ \delta)_j$ $j = i$, $(i+1)$, and $(i-1)$ triggered in the normal operating fashion described in Sec. III. D.	0.85
π^- capture on p	$(\alpha\ \beta\ \gamma\ \delta)_i$	0.34

target to π^0's from a CH target would then be $(2)(290 \pm 40) = 580 \pm 80$, and the π^0's produced per π^- stop in CH would be

$$(1/580 \pm 80)(1.5/2.5) = (1.0 \pm 0.14) \times 10^{-3}.$$

These two measurements are not in agreement. The value of $(3.2 \pm 0.3) \times 10^{-3}$ quoted by Chabre et al. is probably the more reliable and our π^0 efficiency will be based on it. They used their same apparatus to obtain the accepted value of the Panofsky ratio as a check on the systematic errors of their measurement. However, until the number of π^0's per π^- stop in CH is measured by a third party there will remain some doubt.

The $(\alpha\beta\gamma\delta)_i$ rate in our experiment per 10^7 stopped π^-'s is given in Fig. 6. A carbon subtraction has been made by replacing the stopping scintillator with carbon of the same range. The carbon contribution was about 11%. The net average $(\alpha\beta\gamma\delta)_i$ rate is 63 per 10^7 stopped pions.

To calculate the efficiency, a resolution factor is needed to correct for the difference in energy of π^0's from π^+ decay and from π^- capture. The difference in energy causes the angle between the photons to have different distributions. The factor R is defined as the fraction of π^0-decay photon pairs such that if one of the photons hits a counter, the other hits the opposite counter. It is less than unity because of the finite size of the pion stopping distribution and because the angle between the photons is less than 180°. The resolution factors have been calculated by the Monte-Carlo method and are summarized in Table IV. The resolution factor for π^- capture on a proton is low because the angle between the photons may differ from 180° by as much as 23°. A description of the calculation is given in the Appendix.

The π^0 efficiency is then

$$E_{\pi^0} = [(9)(63 \times 10^{-7})/(3.2 \pm 0.3)(10^{-3})](0.85/0.34) = 0.044 \pm 0.004.$$

The factor 0.85 is the resolution factor of the counters for π^0's from π^+ decay and 0.34 is the resolution factor of the counters for π^0's from π^- capture on protons.

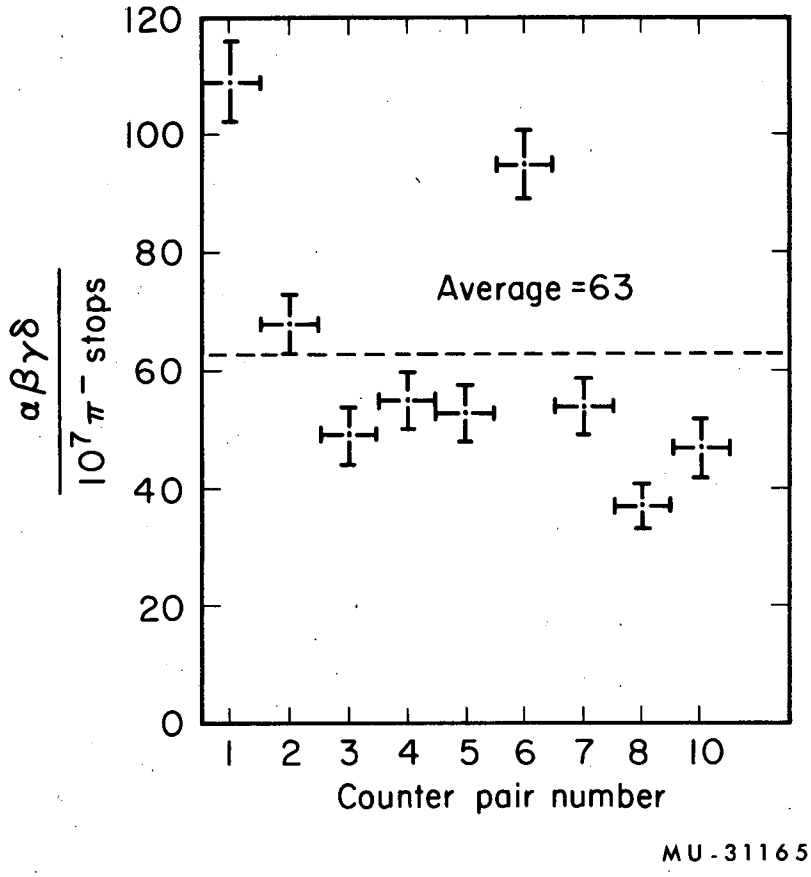

Fig. 6. π^0 counting rate for normal conditions; $\alpha_i\beta_j\gamma_m\delta_n$ trigger and 4 nsec clipping lines on C3.

The π^0 efficiency can also be directly calculated. The actual efficiency of a sandwich counter for a 70 MeV photon will be the product of P_c, the conversion efficiency, and P_f, the efficiency for the electrons to penetrate the next sheet of lead so that a coincidence between the two photo tubes of a counter will occur. The calculated value of P_c is 0.85.

The efficiency for penetrating the following sheet of lead was measured by counting γ-ray coincidences and singles in one of the counters:

$$P_f \text{ for counter } (\gamma\,\delta)_i = \frac{(\alpha\,\beta\,\gamma\,\delta)_i}{(\alpha\,\beta\,\gamma\,\delta)_i + (\alpha\,\beta\,\gamma)_i + (\alpha\,\beta\,\delta)_i} = \frac{(\alpha\,\beta\,\gamma\,\delta)_i}{[\alpha\,\beta\,(\gamma\,U\,\delta)]_i}.$$

The π^0's were made by stopping π^-'s in the stopping counter 5. The data-storage system was triggered by $\alpha_i\,\beta_j\,(\gamma_m\,U\,\delta_n)$ instead of the usual $\alpha_i\,\beta_j\,\gamma_m\,\delta_n$. The 7090 computer then summarized the magnetic-tape data. A carbon subtraction was made. The carbon contributed about 11% of the $(\alpha\,\beta\,\gamma\,\delta)_i$ rate and about 70% of the $(\alpha\,\beta\,\gamma)_i$ and $(\alpha\,\beta\,\delta)_i$ rates. Figure 7 is a plot of $(P_f)_i$ for the 9 sandwich counters in the $\gamma\,\delta$ ring; the average value is $P_f = 0.85$.

In the course of measuring P_f, it was found that the number of fourfold events $(\alpha\,\beta\,\gamma\,\delta)_i$ per π^- stop recorded by the data-storage apparatus was different for a four-fold trigger $\alpha_i\,\beta_j\,\gamma_m\,\delta_n$ and a three-fold trigger $\alpha_i\,\beta_j\,(\gamma_m\,U\,\delta_n)$. The trigger coincidences were formed by the C3 circuit. Figure 6 shows the rate for normal operating conditions. Figure 8 shows the rate with three-fold trigger, increased counter voltages, and longer clipping lines on the C3 circuit. Most of the increase came from the change to a three-fold trigger. The rates were independent of beam level, a strong indication that the difference was not caused by accidentals. We attribute the difference to an electronic loss in the C3 circuit, and introduce an electronic efficiency P_e equal to the ratio of the rates from Figs. 6 and 8:

$$P_e = 63/136 = 0.46.$$

The data from both Figs. 6 and 8 are for captures in the hydrogen of the scintillator; a carbon subtraction of about 11% has been made from both.

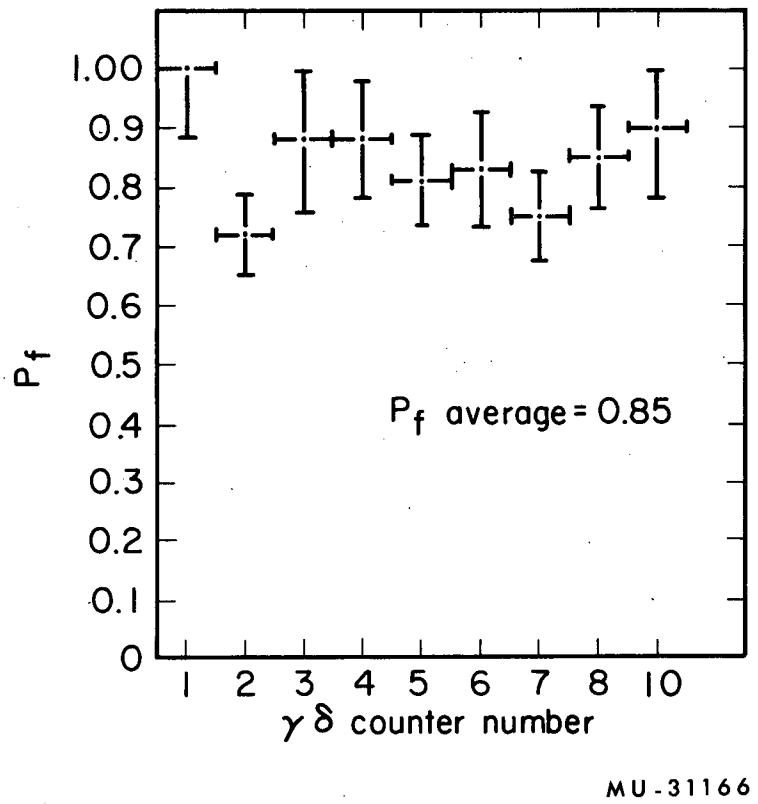

Fig. 7. Efficiency factor P_f; P_f is the probability that one of the electrons will penetrate the next sheet of lead.

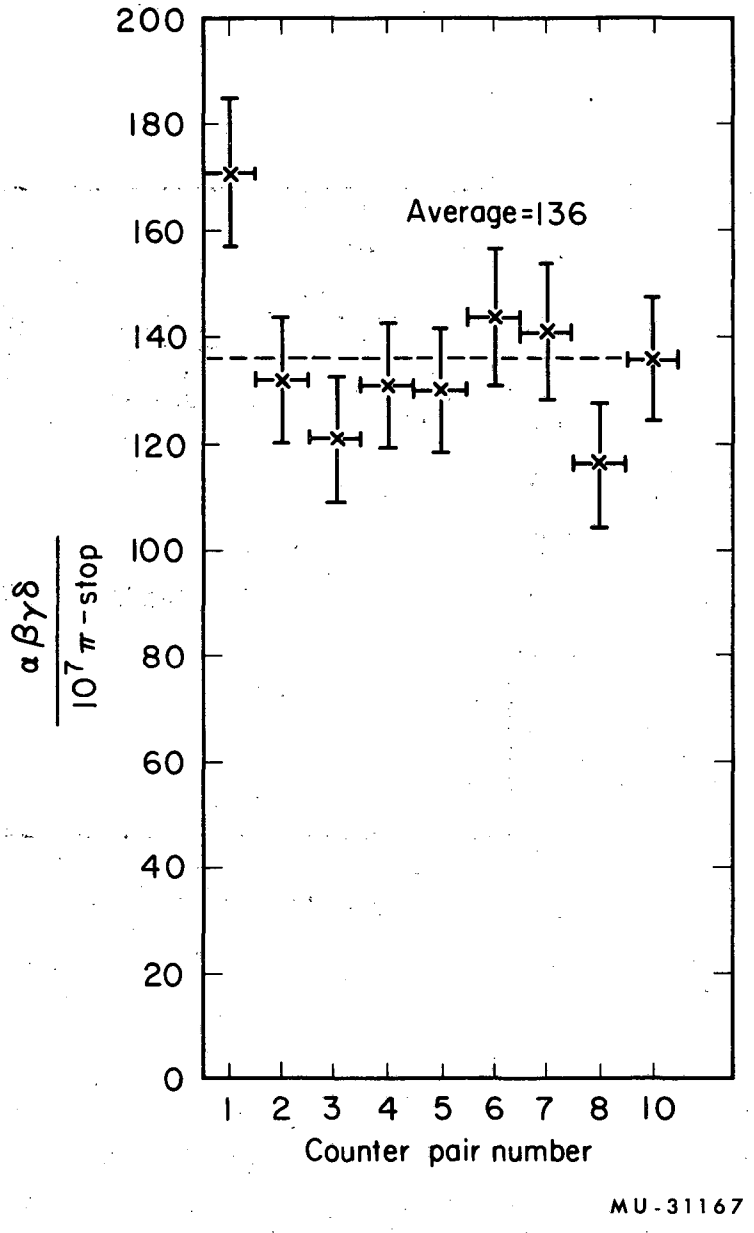

Fig. 8. π^0 counting rate; $\alpha_i\beta_j(\gamma_m U\delta_n)$ trigger, 9 nsec clipping lines on C3, and counter voltages up 100V.

The solid angle of the counter array is

$$\Omega/4\pi = 0.43$$

and this must be multiplied by the resolution factor $R = 0.85$.

The overall calculated efficiency then, for counting a π^0 from π^+ decay, is

$$E_{\pi^0} = (\Omega/4\pi)(R)(P_e)[(P_f)(P_c)]^2 = (0.43)(0.85)(0.46)[(0.85)(0.85)]^2 = 0.088.$$

The most important uncertainty in this number comes from P_e. We do not thoroughly understand the loss and it is possible that P_e is even lower than 0.46. Consequently, the efficiency $E_{\pi^0} = 0.044 \pm 0.004$ obtained from the number of π^0's per π^- capture in CH is used to calculate the $\pi^+ \rightarrow \pi^0$ branching ratio.

D. Annihilation-Photon Efficiency

The efficiency of the 2-in.-thick NaI crystal for 1/2-MeV photons was measured with a Na^{22} source, which emits a 0.54-MeV maximum energy positron and a 1.3-MeV gamma. The Na^{22} source was surrounded by a plastic case which stopped the positrons, creating a source of opposite 1/2-MeV photons with a simultaneous 1.3-MeV gamma. The counter arrangement is illustrated in Fig. 9. A section of the stopping counter, 5C, counted one of the annihilation photons and a second NaI crystal NaI-2, counted the accompanying 1.3-MeV gamma. A tunnel-diode discriminator on the NaI-2 output rejected pulses from 1/2-MeV photons. The NaI-2 crystal and the 5C counter in coincidence triggered the four-beam oscilloscope and camera which recorded the pulses from the NaI annihilation-photon counter. The efficiency was then the number of oscilloscope traces showing an NaI pulse divided by the total number of traces. The result, $P_n = 0.74$, is in good agreement with a calculation from mass absorption coefficients.[27]

A pulse-area distribution was made by measuring 100 of these pulses with a planimeter (see Fig. 10). Ninety per cent of the events had a pulse area between 6 and 22 in an arbitrary unit, and most of the remainder may well have come from 1.3-MeV gammas. We required, therefore, that annihilation photons from positrons in π^+ decay have a pulse height between 6 and 22.

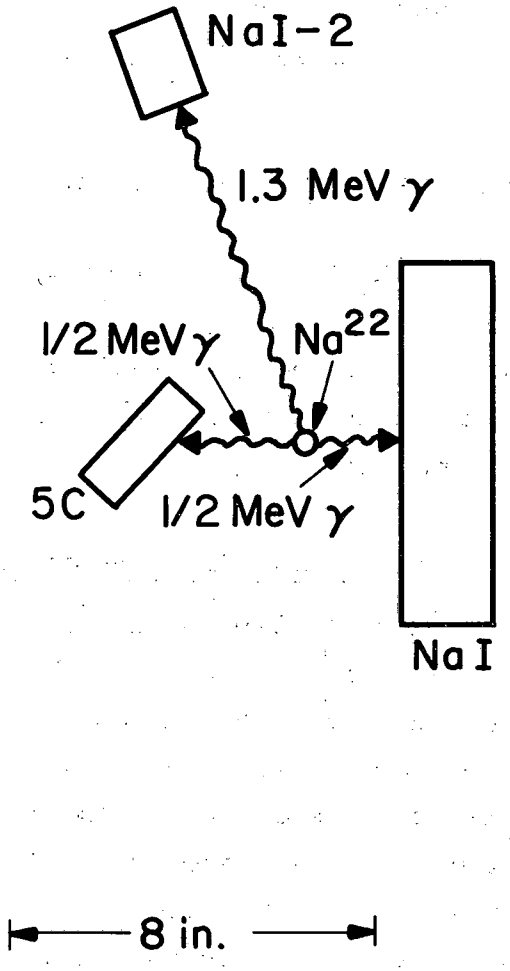

Fig. 9. Measurement of the efficiency of the NaI counter for 1/2 MeV photons.

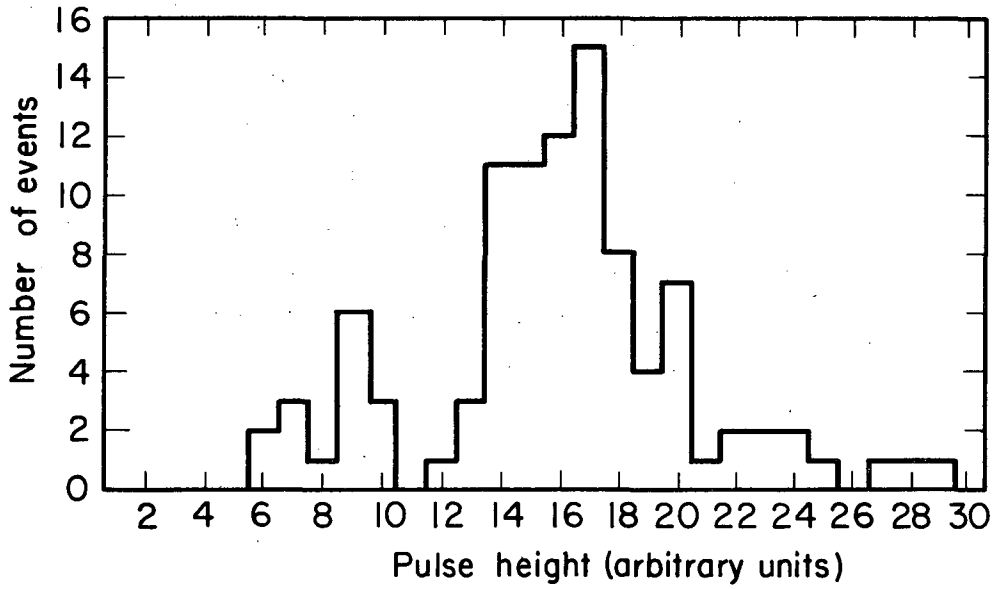

Fig. 10. Pulse-height distribution of 1/2 MeV photons in the NaI counter.

The fraction of annihilation photons lost because they convert before leaving the stopper was measured by putting a 1.5-in. -thick scintillator between the Na^{22} source and the NaI annihilation-photon counter. The efficiency factor for this effect is $P_L = 0.78$.

A correction might be expected for those positrons which escaped the stopper before annihilating. However, a calculation has been made which shows this loss to be less than 3%.

Another correction, this one important, had to be made to correct for the loading of the annihilation counter by beam particles. Saturating pulses were about 1.0 μsec long, and 1/2-MeV pulses were about 0.8 μsec. If the counter was already occupied at the time of an event, the event would be missed. The requirement was made that no second pulse disturb the annihilation pulse. To measure the loss caused by this requirement, the oscilloscope was triggered as usual but set for a very slow sweep speed, 1.0 μsec/cm, and the unoccupied fraction of the trace measured. The result, $P_s = 0.70$, agreed with the fraction of triggers during the π^+ decay measurement that were rejected because the NaI oscilloscope trace was disturbed.

The solid-angle factor for the NaI counter was

$$\Omega/2\pi = 0.35.$$

The total annihilation-photon efficiency was therefore

$$E_\gamma = (\Omega/2\pi)\, P_n P_L P_s = (0.35)(0.74)(0.78)(0.70) = 0.14.$$

E. Positron Efficiency

The efficiency for recognizing a positron in the stopper is estimated to be about 0.51. The pulse in the counter in which the π^+ stopped was usually 15 to 20 nsec long, and the positron had to be seen on the tail of this pulse to be recognized at earlier times.

A $\pi^+ \rightarrow \mu^+ + \nu$ lifetime curve taken with the stopping counter is shown in Fig. 11. The oscilloscope was triggered to record each pion stop, and a very low beam was employed. The point at zero time was obtained by assuming for those events in which a muon was not visible

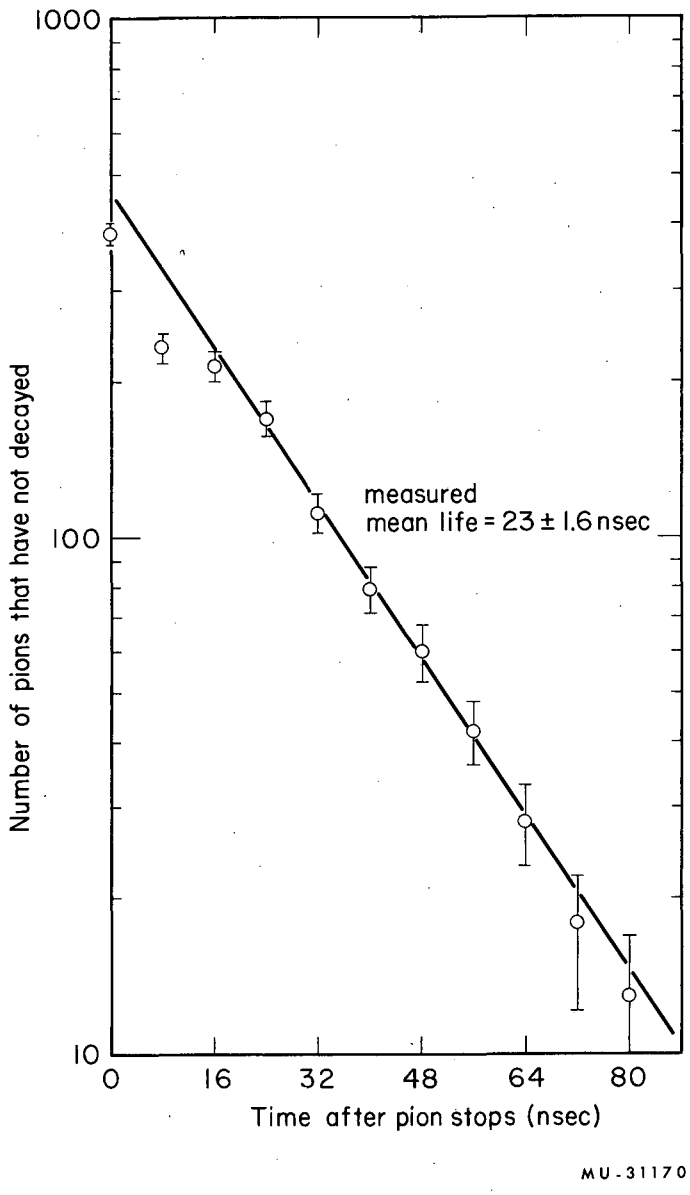

Fig. 11. π^+ lifetime curve.

that the muon came too early to be seen. The lifetime curve indicates, incidently, that no appreciable number of muons or positrons were counted as pions because if they were, the point at time zero would be above the extrapolated lifetime curve. Figure 12 shows the same data plotted in a differential form. Muons that came earlier than about 16 nsec are missed. Of the pion decays within the gate, 0.55 of them occur later than 16 nsec. This fraction of the positrons would be recognized provided their pulse height were large enough. A 2-mm deflection on the viewer corresponds to a 1/2-MeV positron and would have been seen. From a phase-space calculation, 0.93 of the positrons have a kinetic energy greater than 1/2 MeV. The positron efficiency is therefore

$$E_p = (0.55)(0.93) = 0.51.$$

F. Miscellaneous Factors

Events may have been lost through an accidental count in one of the ten large anticounters $A_{1....10}$. The frequency of counts was observed on the film data, and from the measured resolution of the anticoincidence circuit, the loss is estimated to be about 8%.

Occasionally during the experiment the beam spill would "spike." The π's would come bunched in time so that the instantaneous rate would be very large. If a real event occurred during a beam spike the film would be unreadable. The estimated loss is 5%.

G. Uncertainty in the Efficiency

The 10% uncertainty in the π^0 efficiency is combined with estimates of the uncertainty in other efficiency factors to give a total efficiency uncertainty of 30%. This uncertainty is small enough that the error assigned the branching ratio is dominated by the statistical uncertainty in the number of events.

The efficiency makes use of the number of π^0's per π^- stop in CH measured by Chabre et al. $[(3.2 \pm 0.3) \times 10^{-3}]$. If this number should prove incorrect, the branching ratios should be scaled accordingly.

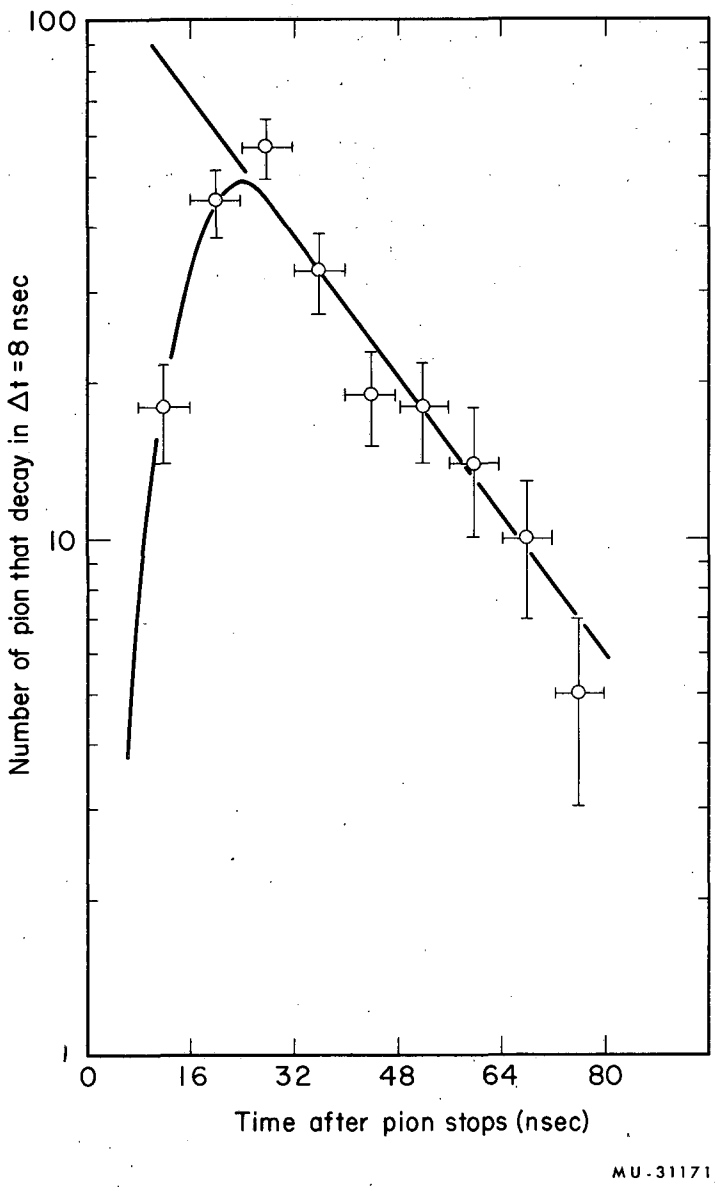

Fig. 12. Differential π^+ lifetime curve.

IV. RESULTS AND ANALYSIS

A. Events

During the data run, 5.6×10^{10} pions were stopped in counter 5, as measured by the C2 coincidence circuit. The stopping pion rate was 10^5 per sec. Thirty thousand of these stopped pions triggered the data-storage system, so the trigger rate was about 5 per 10^7 stopped pions. The stored events were conveniently divided into four groups according to the location of the active counters with respect to each other. The following list shows this division, the name assigned each group, and the percentage of the stored events in each group:

Name	Type of Event	Percentage
Opposite	$(\alpha\beta\gamma\delta)_i$	11
Fork	$(\alpha\beta)_i(\gamma\delta)_{j=i\pm1}$	13
Wide Fork	$(\alpha\beta)_i(\gamma\delta)_{j=i\pm2}$	46
Junk	All events other than the three types above	30

One extra, odd counter was permitted to register in the first three groups. The distribution of events is shown in Table V.

Good events from pion-beta decay are most likely to be in the Opposite group. However, because of the finite size of the stopping pion distribution, and the 3.8° possible deviation from 180° of the π^0 decay photons, good pion-beta-decay events may also be found in the Fork group. The expected distribution of good events between the Opposite and Fork groups was calculated in the Monte-Carlo calculation described in Sec. III C. The result is 8 to 1 in favor of the Opposite group. Wide-Fork events are interesting because they could not come from pion-beta decay and therefore serve as a monitor of background. The angle between the two photons for Wide-Fork events is too far from 180°.

Table V. Distribution of stored events of type $(\alpha\beta)_i (\gamma\delta)_j$ for 10% of the data. The shaded areas were excluded by the coincidence system. Possibly good events must lie on the diagonal or one away from the diagonal. The enclosed areas contain events that could not come from pion-beta decay and are used to estimate the background. Counters that would have been in the 9 position were omitted to make room for the pion beam.

αβ \ γδ	1	2	3	4	5	6	7	8	9	10
1	33	25	41	46						50
2	16	15	16	28						56
3	60	16	16	28						76
4	109	43	20	40						174
5					28	41	41	110		
6					21	33	18	121		
7					42	25	13	54		
8					86	89	21	45		
9										
10	73	92	121	97						115

Most of the data-storage triggers must have come from charge exchange π^0's which were made either in the beam-counter telescope or absorber by a pion which arrived during the gate generated by the preceding pion. The effect of putting the $\alpha\beta$ counters out of delay with the $\gamma\delta$ counters was to reduce the trigger rate to essentially zero, indicating that the triggers were caused by "real" events. The number of data-storage triggers per stopped pion was found to be directly proportional to the pion-beam rate, as expected if the data storage triggers were caused by the charge exchange of a second unrelated pion.

For about 2% of the pion stops there was another pion in the same rf pulse, and for another 2% of the stops there was another pion in the next rf pulse. The delayed gate and the $\overline{1D}$ veto were intended to eliminate triggers from these second pions, and they did help. The $\overline{1D}$ veto reduced the trigger rate by 50%, and the 1 pulse displayed on the 4-beam oscilloscope permitted the immediate elimination of another 17% of the events. However, the 1 pulse was about 50 nsec long and a second pulse that occurred within the first 30 nsec did not always stand out clearly enough to be recognizable.

Dunaitsev et al.[30] have measured the charge-exchange cross section for π^+'s on carbon at 150 MeV/c and several lower momenta. A rough calculation indicates that all of our data-storage triggers can be attributed to charge exchange. Since most of the triggers of the Opposite, Fork, and Wide-Fork groups undoubtedly came from the same source, a study of Wide-Fork events should be a good measure of the background.

B. Film Analysis

We scanned the film for all 30,000 recorded events for a NaI signal without referring to which gamma counters caused the event. In the initial scan, time agreement between the NaI pulse and the π^0 gamma counters within about 15 nsec was required, and the NaI signal was ignored if it clearly came promptly after the pion stopped, or if there was a counter 7 veto in time with it. Two hundred and two events were found and their distribution in the four groups is given in the first

column of Table VI. This table shows the effect of progressively applying the criteria of a good event.

The timing criteria were that the rms deviation of the times of the four π^0 counters from their average be less than 4 nsec, and that their average time agree with the NaI counter within ± 6 nsec. These requirements were decided upon after studying film events made by prompt π^0's from stopping π^-'s. Essentially all of these prompt events had an rms deviation from their individual averages of less than 4 nsec. The rms deviation of the average of the four π^0 counter times from the overall average which set the zero time markers was 1.8 nsec. These time deviations were principally caused by jitter in the arrival time of the counter signals although they do also include human measuring jitter. An examination of the film taken to measure the NaI efficiency indicated that its time could be easily measured within ± 6 nsec. Timing between the electron and the average of the π^0 counters was required within ± 4 nsec. These timing criteria are believed to introduce no loss in efficiency.

The NaI pulse area was required to be between 6 and 22 in the arbitrary units used in Fig. 10. Most of the pulses satisfying this requirement were somewhat smoother than the very jagged pulses from the Na^{22} calibration. Some were very smooth, especially those that began soon after another pulse finished. Photoelectron statistics were responsible for the Na^{22} calibration pulses being jagged. Probably the pulses on the tail of another were smooth because the counter was badly loaded and needed some time to recover between pulses. Approximately 200 nsec of time prior to the NaI pulse was displayed on the four-beam oscilloscope, so the requirement was made that the trace be undisturbed for this time. This is a straightforward procedure and reduces the efficiency by a measurable amount. However, some of the remaining pulses were also very smooth. These have been eliminated in the lower part of Table VI. This final elimination of smooth pulses is probably valid because it is unlikely that they come from 1/2-MeV photons. Nevertheless, the elimination is a somewhat subjective procedure.

Table VI. Good-event criteria applied progressively; π, N, and e refer respectively to the average time of the π^0 counters, the NaI time, and the time of a second pulse in the stopping counter. In the lower half of the table, the very smooth NaI pulses are eliminated before the final two columns.

Type of event	Number stored	Initial scan: $\lvert N-\pi \rvert < 15$ nsec, N not prompt, no 7	$\lvert N-\pi \rvert < 6$ nsec Δ rms $\pi < 4$ nsec	NaI pulse area 6 to 22	NaI pulse not on the tail of another		No muon ($\lvert \pi-e \rvert > 4$ nsec)	With electron ($\lvert \pi-e \rvert < 4$ nsec)
Opposite	3200	30	18	10	7		5	2
Fork	4000	41	26	11	8		6	3
Wide Fork	13,800	74	36	10	9		4	2
Junk	9000	57	25	5	4		0	0
Total	30,000	202	105	36	28			
						NaI pulse not smooth		
Opposite	3200	30	18	10	7	7	5	2
Fork	4000	41	26	11	8	6	4	3
Wide Fork	13,800	74	36	10	9	6	2	1
Junk	9000	57	25	5	4	2	0	0
Total	30,000	202	105	36	28			

Four of the remaining events in both the top and bottom part of Table VI were eliminated because they had a second pulse in the stopping counter out of time with the π^0 counters and within 100 nsec of the stopped pion. These pulses were attributed to $\pi^+ \rightarrow \mu^+ + \nu$ decay. While it is possible that the positron pulse in pion-beta decay will not be seen, a muon pulse should definitely not be present. To demonstrate that these out-of-time pulses are actually muons from the stopped pion, the lifetime of pulses following the stopping pion pulse was measured for a sample of the total stored events and found to agree with the pion lifetime.

The possibly good events in Table VI are listed in Table VII. The times given for the decays are consistent with the known pion lifetime of 25.5 nsec. It might appear possible to actually calculate the lifetime of these events and compare it to the pion lifetime; however, the short gate time of 40 nsec combined with the small number of events makes the error extremely large.

C. Background

The background can be estimated in several ways. The number of Wide-Fork events may be scaled in proportion to the number of stored events. For example, there are approximately 4 times as many Wide-Fork as Opposite stored events. The backgroun to the 5 Opposite events would be the 4 Wide-Fork events divided by 4, or 1. If the smooth events are eliminated as in the lower part of the table, the estimated background to the 5 Opposite events is 1/2.

Another indication of background is the number of events eliminated for having a decay muon from the pion. The efficiency for detecting the muon was about 1/2, the reduction from unity being chiefly caused by those muon pulses that came early and were lost in the large stopping pion pulse. Consequently, a number of events, equal to the number eliminated for having a muon, are expected to have a muon too early to be seen. The background estimated in this way is 2 in the 5 Opposite events.

Table VII. Events which satisfy the oscilloscope-display criteria for a good event.

	π^0 counters	Time (nsec)	NaI pulse area (units of Fig.10)	Electron pulse height (mm)
Opposite				
	$(\alpha\beta\gamma\delta)_3$	8	13	--
	$(\alpha\beta\gamma\delta)_{10}$	26	9	3
	$(\alpha\beta\gamma\delta)_{10}$	19	8	--
	$(\alpha\beta\gamma\delta)_8$	19	10	--
	$(\alpha\beta\gamma\delta)_5\delta_4$	11	9	4
Fork				
	$(\alpha\beta)_1(\gamma\delta)_{10}$	30	15	--
	$(\alpha\beta)_1(\gamma\delta)_{10}$	35	7	4
	$(\alpha\beta)_5(\gamma\delta)_6$	27	10	5
	$(\alpha\beta)_7(\gamma\delta)_8$	23	8	5
	$(\alpha\beta)_{10}(\gamma\delta)_1\alpha_6$	42	6 (smooth)	--
	$(\alpha\beta)_{10}(\gamma\delta)_1$	31	22 (smooth)	--
Wide Fork				
	$(\alpha\beta)_2(\gamma\delta)_4\gamma_7$	16	21	--
	$(\alpha\beta)_2(\gamma\delta)_{10}$	33	6	8
	$(\alpha\beta)_7(\gamma\delta)_5$	29	20 (smooth)	4
	$(\alpha\beta)_5(\gamma\delta)_7\delta_{10}$	31	8 (smooth)	--

The background can also be calculated from Table VIII, where the criteria of a good event are applied independently to the entire sample, rather than consecutively. In the 202 events from the initial scan, there are 76 with acceptable NaI pulses, (including the smooth pulses) and the fraction of these expected to be in time with the π^0 counters is 105/202. The fraction expected to show an "electron" or "neither electron nor muon" (no second pulse in the stopper unless the second pulse is in time with the π^0 counters) is (32+74)/202 = 106/202. The overall background in 30,000 events is therefore

$$(76)(105/202)(106/202) = 21,$$

and the contribution to the Opposite events is (21)(3200/30000) = 2.2.

The ratio of Opposite to Fork events also indicates background. Since a ratio of 8 to 1 is expected, it is very unlikely that we measure 5 to 6 or even 5 to 4 in the absence of background.

There is certainly a possibility that all the events are background. The Poisson probability of seeing 5 or more background events when 2 are expected is 5%. Ninty-five percent may be taken as an estimate of the reliability with which the pion beta decay has actually been observed.

D. Branching Ratio

Table IX gives the branching ratio for progressively more restrictive criteria. The $(\alpha\beta\gamma\delta)_{10}$ counters have been excluded in the lowest part of the table because their trigger rate was so much larger than the other π^0 counters (see Table V). The $(\alpha\beta\gamma\delta)_{10}$ and the $(\alpha\beta\gamma\delta)_8$ counters were closest to the pion beam, and this probably is the reason for the higher trigger rate.

The criteria that lead to the branching ratio $(2.1^{+1.9}_{-1.2})\times 10^{-8}$ are probably sufficiently restrictive. This result is consistent with the prediction of the CVC theory. However, the statistical accuracy is not good. A precise measurement of this branching ratio (10 per cent or better) would still be very valuable.

Table VIII. Good-event criteria applied independently.

Type of event	Number stored	Initial scan: $\lvert N-\pi \rvert < 15$ nsec, N not prompt, no 7	$\lvert N-\pi \rvert \lesssim 6$ nsec, Δ rms < 4 nsec	NaI pulse area 6 to 22	NaI pulse area 6 to 22, and not on the tail of another	NaI pulse area 6 to 22, not on tail of another, and not smooth	Muon ($\lvert \pi-e \rvert > 4$ nsec)	Electron ($\pi-e$ $\lvert <$ 4 nsec)	Neither muon nor electron
Opposite	3200	30	18	16	13	9	13	9	8
Fork	4000	41	26	10	16	12	17	8	16
Wide Fork	13,800	74	36	31	30	20	37	6	31
Junk	9000	57	25	19	17	8	29	9	19
Total	30,000	202	105	86	76	49	96	32	74

Table IX. Branching ratio for pion-beta decay: $(\pi^+ \to \pi^0 + e^+ + \nu)/(\pi^+ \to \mu^+ + \nu)$

π^0 counters $(\alpha\beta)_i(\gamma\delta)_j$	e^+ detected by	Acceptable events	Estimated background	Efficiency (%)	Branching ratio ($\times 10^{-8}$)
$i = j \pm 0, 1$	NaI	11	2 to 4	0.35 ± 0.12	4.1 ± 2.2
$i = j$	NaI	5	1 to 2	0.32 ± 0.10	$1.9^{+1.9}_{-1.2}$
$i = j$	NaI and 5	2	1/2	0.16 ± 0.05	$1.7^{+2.7}_{-1.4}$
$i = j \pm 0, 1$	NaI[a]	9	1 to 4	0.35 ± 0.12	3.3 ± 2.0
$i = j$	NaI[a]	5	1/2 to 2	0.32 ± 0.10	$2.1^{+1.9}_{-1.2}$
$i = j$	NaI[a] and 5	2	1/4	0.16 ± 0.05	$1.9^{+2.7}_{-1.4}$
$i = j \pm 0, 1$[b]	NaI[a]	5	1/2 to 2	0.32 ± 0.10	$2.1^{+1.9}_{-1.2}$
$i = j$[b]	NaI[a]	3	1/4	0.28 ± 0.08	$1.7^{+1.8}_{-1.0}$
$i = j$[b]	NaI[a] and 5	1	--	0.14 ± 0.04	$1.3^{+1.5}_{-0.9}$

[a] The smooth NaI pulses are excluded.

[b] The i = 10 counters are excluded.

ACKNOWLEDGMENTS

I thank Professor Thomas Ypsilantis for his excellent guidance during this work. Particular thanks are due Dr. Clyde Wiegand for his many contributions to the design and operation of the experiment. Dr. Rudolf Larsen has been a source of encouragement and assistance during my entire graduate career, and the help of Dr. Tom Elioff has been invaluable. The continued support and consul of Professor Emilio Segrè is also deeply appreciated.

I also thank Mr. Joseph Good for his programming assistance and Mr. Cedric Larson for the design of the mechanical support for the experimental apparatus. The assistance of the 184-inch cyclotron crew under Mr. James Vale and of the accelerator technicians is also gratefully acknowledged.

This work was done under the auspices of the U. S. Atomic Energy Commission.

APPENDIX

Monte Carlo Calculation of the π^0 Resolution Factor.

The calculation was begun by selecting the pion stopping coordinates according to Gaussian distributions in each of the three dimensions. For example, x is selected according to

$$P(x) = \frac{1}{(2\pi\sigma)^{1/2}} \exp - \frac{x^2}{2\sigma^2}.$$

Perpendicular to the beam, $\sigma = 1.5$ in., and was measured by small beam profile counters. Along the beam $\sigma = 0.85$ in., and was found by noting the relative frequency of π^+ stops in 5A, B, and C. Actually, the calculation is not particularly sensitive to the exact stopping distribution. To select x according to a probability P(x), one solves the equation (for x)

$$\int_{x_{min}}^{x} P(\xi) d\xi = N,$$

where N is a random number between 0 and 1, and P(x) is, of course, normalized to 1:

$$\int_{x_{min}}^{x_{max}} P(\xi) d\xi = 1.$$

An element of solid angle $d\Omega(\theta, \phi)$ is chosen for one of the γ rays, and if it hits a certain counter, the calculation proceeds; otherwise, it starts over again for another try. If it hits, angles for the second γ ray are selected, and a calculation is made to find whether or not the second hits the γ ray counter opposite to the counter hit by the first γ ray. In selecting these angles, the π^0 energy is taken into account. The angle between the two γ rays is then, in general, less than 180 deg.

It is selected by choosing at random an element of solid angle for the γ rays in the center-of-mass system of the π^0, and then transforming it to the laboratory system. The ratio of the number of tries where the second photon hits the opposite counter to those where it does not, gives the resolution factor R.

FOOTNOTES AND REFERENCES

1. R. P. Feynman and M. Gell-Mann, Phys. Rev. 109, 193 (1958).
2. S. Gershtein and I. Zeldovitch, Soviet Phys. JETP (Engl. Transl.) 2 576 (1956).
3. R. K. Bardin, C. A. Barnes, W. A. Fowler, and P. A. Seeger, Phys. Rev. 127, 583 (1962).
4. Hans A. Weidenmüller, Phys. Rev. 127, 537 (1962).
5. Enrico Fermi, Nuclear Physics (University of Chicago Press, Chicago, 1950), p. 76.
6. W. H. Barkas and A. H. Rosenfeld, Data for Elementary Particles, Lawrence Radiation Laboratory Report UCRL-8030 Rev., Oct. 1 1961 (unpublished).
7. G. Da Prato and G. Putzolu, Nuovo Cimento 21, 541 (1961).
8. E. Feenberg and H. Primakoff, Phil. Mag. 3, 321 (1958).
9. Ya. B. Seldovich, Doklady Akad. Nauk, SSSR 97, 421 (1954).
10. Private communication, Dr. S. M. Berman, SLAC, Stanford, California.
11. T. Mayer-Kuckuk and F. C. Michel, Phys. Rev. 127, 545 (1962).
12. Murray Gell-Mann, Phys. Rev. 111, 363 (1958).
13. F. Boehm, V. Soergel, and B. Stech, Phys. Rev. Letters 1, 77 (1958).
14. M. E. Nordberg, Jr., F. B. Morinigo, and C. A. Barnes, Phys. Rev. 125, 321 (1962).
15. T. Fazzini, G. Fidecaro, A. W. Merrison, H. Paul, and V. A. Tollestrup, Phys. Rev. Letters 1, 247 (1958).
16. P. Depommier, J. Heintze, A. Mukhin, C. Rubbia, V. Soergel, and K. Winter, Phys. Rev. Letters 2, 23 (1962).
17. A. Dunaitsev, V. Petrukhin, Yu. Prokoshkin, and V. Rykalin, Phys. Letters 1, 138 (1962).
18. S. De Benedetti and H. C. Corben, Positronium, in Ann. Rev. Nucl. Sci. 4, (1954), p. 191.
19. Bruno Rossi, High-Energy Particles (Prentice-Hall, Inc., New York, 1952).

20. R. R. Wilson, Phys. Rev. 86, 261 (1952).

21. The magnet system was designed principally by Dr. R. A. Swanson.

22. The electronics for this measurement were built by Arthur E. Bjerke and Thomas A. Nunamaker. A very fast tunnel-diode-type coincidence circuit, and tunnel-diode-discriminated photo-tube signals were employed.

23. Arthur E. Bjerke, Quentin A. Kerns, and Thomas A. Nunamaker, "Pulse Shaping and Standardization of Photomultiplier Signals for Optimum Timing Information Using Tunnel Diodes," Lawrence Radiation Laboratory Report UCRL-9838, Aug. 30, 1961.

24. Clyde E. Wiegand, in Proceedings of an International Conference on Instrumentation for High-Energy Physics (Interscience Publishers, Inc., New York, 1960), p. 182.

25. F. Evans and F. A. Kirsten, Nucl. Instr. Methods 12, 39 (1961).

26. Quentin A. Kerns and Gerald C. Cox, Nucl. Instr. Methods 12, 32 (1961).

27. A. F. Dunaitsev, V. I. Petrukhin, Yu. D. Prokoshkin, and V. I. Rykalin, Soviet Phys. JEPT (Engl. Transl.) 15, 439 (1962).

28. M. Chabre, P. Depommier, J. Heintze, and V. Soergel (submitted to Physics Letters).

29. J. Ashkin, T. Fazzini, G. Fidecaro, Y. Goldschmidt-Clermont, N. H. Lipman, A. W. Merrison, and H. Paul, Nuovo Cimento 16, 490 (1960).

30. A. F. Dunaitsev, V. I. Petrukhin, Yu. D. Prokoshkin, and V. I. Rykalin, 1962 International Conference on High Energy Physics at CERN, p.12.

31. C. E. Crouthamel, Applied Gamma-Ray Spectrometry, Pergamon Press, New York 1960, p. 99.